Long non-coding RNA small nucleolar RNA host gene 6 aggravates pancreatic cancer through upregulation of far upstream element binding protein 1 by sponging microRNA-26a-5p

Xing-Xing Zhang[1], Hua Chen[1], Hui-Ying Li[1], Rui Chen[1], Lei He[1], Juan-Li Yang[1], Lin-Lin Xiao[2], Jin-Lian Chen[1]

[1]Department of Gastroenterology, Shanghai University of Medicine & Health Sciences Affiliated Sixth People's Hospital South Campus, Shanghai 201499, China;
[2]Department of Laboratory Medicine, Shanghai University of Medicine & Health Sciences Affiliated Sixth People's Hospital South Campus, Shanghai 201499, China.

Abstract

Background: Pancreatic cancer (PC) is a highly deadly malignancy with few effective therapies. We aimed to unmask the role that long non-coding RNA small nucleolar RNA host gene 6 (*SNHG6*) plays in PC cells by targeting far upstream element binding protein 1 (*FUBP1*) via microRNA-26a-5p (*miR-26a-5p*).

Methods: *SNHG6* expression was predicted by bioinformatics, followed by verification via reverse transcription quantitative polymerase chain reaction. Then, the interactions among *SNHG6*, *miR-26a-5p*, and *FUBP1* were detected through online software analysis, dual luciferase reporter assay and RNA pull-down. After that, cells were treated with different small interfering RNAs and/or mimic to determine the interactions among *SNHG6*, *miR-26a-5p*, and *FUBP1* and their roles in PC cells. Finally, the role of *SNHG6* in tumor growth *in vivo* was evaluated by measuring the growth and weight of transplanted tumors in nude mice. A *t*-test, one-way and two-way analysis of variance were used for data analysis.

Results: Compared with that in normal tissues, *SNHG6* was highly expressed in PC tissues (1.00 ± 0.05 *vs.* 1.56 ± 0.06, $t = 16.03$, $P < 0.001$). Compared with that in human pancreatic duct epithelial cells (HPDE6-C7), *SNHG6* showed the highest expression in PANC-1 cells (1.00 ± 0.06 *vs.* 3.87 ± 0.13, $t = 34.72$, $P < 0.001$) and the lowest expression in human pancreatic cancer cells (MIAPaCa-2) (1.00 ± 0.06 *vs.* 1.41 ± 0.07, $t = 7.70$, $P = 0.0015$). Compared with the levels in the si-negative control group, *SNHG6* (0.97 ± 0.05 *vs.* 0.21 ± 0.06, $t = 16.85$, $P < 0.001$), N-cadherin (0.74 ± 0.05 *vs.* 0.41 ± 0.04, $t = 8.93$, $P < 0.001$), Vimentin (0.55 ± 0.04 *vs.* 0.25 ± 0.03, $t = 10.39$, $P < 0.001$), and β-catenin (0.62 ± 0.05 *vs.* 0.32 ± 0.03, $t = 8.91$, $P < 0.001$) were decreased, while E-cadherin (0.65 ± 0.06 *vs.* 1.36 ± 0.07, $t = 13.34$, $P < 0.001$) was increased after *SNHG6* knockdown or *miR-26a-5p* overexpression, accompanied by inhibited cell proliferation, migration, and invasion. *SNHG6* overexpression exerted the opposite effects. *SNHG6* upregulated *FUBP1* expression by sponging *miR-26a-5p*. Silencing *SNHG6* blocked the growth of PC *in vivo*.

Conclusion: Silencing *SNHG6* might ameliorate PC through inhibition of *FUBP1* by sponging *miR-26a-5p*, thus providing further supporting evidence for its use in PC treatment.

Keywords: Prostatic neoplasms; Long non-coding RNA *SNHG6*; microRNA-26a; *FUBP1*; Proliferation; Invasion; Migration; Apoptosis

Introduction

Pancreatic cancer (PC) is a severe malignancy in the digestive system characterized by aggressive clinical behavior, rapid expansion, and poor prognosis.[1] PC may be caused by an increased serum concentration of free insulin-like growth factor, stimulating the growth of pancreatic cells in the long term.[2] PC has been demonstrated to be one of the most deadly diseases with few available interventions and with less than 5% 5-year overall survival.[3] PC is generally diagnosed at an early stage and is resistant to known anti-cancer drugs.[4] Despite some diagnostic and therapeutic improvements, the mortality of PC has remained almost the same over the past several decades, partly due to a lack of screening methods and markers for early diagnosis.[5] Therefore, it is of great importance to identify the underlying molecular mechanisms of the carcinogenesis and progression of PC and to explore novel therapeutic and diagnostic targets for PC treatment.

Long non-coding RNAs (lncRNAs) have been reported to be involved in many biological processes and their deregulation is associated with cancer development.[6]

Access this article online

Quick Response Code:

Website: www.cmj.org

DOI: 10.1097/CM9.0000000000000758

Correspondence to: Prof. Jin-Lian Chen, Department of Gastroenterology, Shanghai University of Medicine & Health Sciences Affiliated Sixth People's Hospital South Campus, No. 6600 Nanfeng Road, Fengxian District, Shanghai 201499, China
E-Mail: drchenjinlian0621@163.com

Chinese Medical Journal 2020;133(10)

Received: 09-01-2020 **Edited by:** Peng Lyu

As one of the housekeeping genes in the 5′-terminal oligopyrimidine tract family, lncRNA small nucleolar RNA host gene 6 (*SNHG6*) is associated with ribosomes.[7] Different cancers, such as breast cancer, colorectal cancer, osteosarcoma, and PC, have been reported to be correlated with *SNHG6*.[8-11] A previous study demonstrated that microRNA (miR) expression can affect normal biological processes in pancreatic cells, resulting in tumor occurrence and progression.[12] microRNA-26a-5p (*miR-26a-5p*) plays a role in the occurrence and development of several tumors, including papillary thyroid carcinoma, osteosarcoma, and breast cancer.[11,13,14] *SNHG6* has also been found to affect cancer cells through regulation of *miR-26a-5p* in breast cancer and lung adenocarcinoma.[15,16] Interestingly, *miR-26a* has been revealed to participate in PC in different studies.[17,18] However, the specific roles of *SNHG6* and *miR-26a-5p* in PC progression remain to be elucidated.

Bioinformatics analysis and dual luciferase reporter assays in our study showed that there are interactions among *SNHG6*, *miR-26a-5p* and far upstream element binding protein 1 (*FUBP1*) in PC. *FUBP1* could control mRNA transcription of its target genes via the single-stranded DNA element far upstream element and interactions with the basal transcriptional machinery.[19] A previous study confirmed that a high level of *FUBP1* is associated with a significant reduction in PC patient survival.[20] Based on these studies, we aimed to investigate the relationships among *SNHG6*, *miR-26a-5p*, and *FUBP1* in the course of PC development. Moreover, we mainly discuss the effects of *SNHG6* on PC cell progression.

Methods

Ethics statement

All participants signed informed consent forms. The study was officially approved by the Ethics Committee of Shanghai University of Medicine & Health Sciences Affiliated Sixth People's Hospital South Campus (No. 2017-Ethical review-KY-05). The animal experiments were conducted based on a minimal animal number and the least pain on experimental animals.

Tissue samples

From September 2017 to September 2018, patients diagnosed with PC at the Shanghai University of Medicine & Health Sciences Affiliated Sixth People's Hospital South Campus were enrolled in this experiment. Five pairs of PC and adjacent normal tissues (at least 3 cm away from the margin of PC tissues) were resected and collected. None of the patients received radiotherapy or chemotherapy before the operation and all were diagnosed with PC by pathological examination after the operation. Patients with chronic system diseases or other malignant tumors were excluded.

Cell culture

PC cell lines (MIAPaCa-2, BxPC-3, Capan-1, and Panc-1) and the human normal pancreatic ductal epithelial cell line (HPDE6-C7) were obtained from the American Type Culture Collection (ATCC, Rockville, MD, USA). Cells were cultured in Dulbecco modified Eagle medium (DMEM) (Gibco, Grand Island, NY, USA) with 10% fetal bovine serum (FBS, Beijing Solarbio Science & Technology Co., Ltd., Beijing, China) and 1% penicillin and streptomycin at 37°C with 5% CO_2. When PC cell confluence reached approximately 80%, PC cells were subcultured. After stable subculture for 2 to 3 passages, the expression of *SNHG6* in cells at the logarithmic phase was measured.

Cell treatment

SNHG6 was downregulated using small interfering RNA (siRNA) in the Panc-1 cell line. The Panc-1 cell line was treated with siRNA negative control (si-NC), si-*SNHG6*-1, or si-*SNHG6*-2, or it was left untreated (blank group). *SNHG6* in the MIAPaCa-2 cell line was upregulated by treatment with the pCD513B-1 overexpression plasmid. The MIAPaCa-2 cell line was treated with the pCD513B-1 NC plasmid (LV-NC group), pCD513B-1-*SNHG6* plasmid (LV-SNHG6 group), or it was left untreated (blank group). The *miR-26a-5p* expression in MIAPaCa-2 cells was upregulated. The MIAPaCa-2 cell line was treated with mimic NC (mimic NC group), *miR-26a-5p* overexpression plasmid (*miR-26a-5p* mimic group), or it was left untreated (blank group). In addition, the MIAPaCa-2 cell line was co-treated with pCD513B-1-*SNHG6* + mimic NC or pCD513B-1-*SNHG6* + *miR-26a-5p* mimic. Transient cell transfection was performed strictly according to the Lipofectamine™ 2000 kit instructions (Invitrogen, Carlsbad, CA, USA). After 48 h, the transfection efficiency was verified through detection of *SNHG6* expression via reverse transcription quantitative polymerase chain reaction (RT-qPCR) and western blot analysis. The si-NC, si-*SNHG6*-1, si-*SNHG6*-2, pCD513B-1 plasmid, mimic NC, and *miR-26a-5p* mimic were designed and synthesized by Guangzhou RiboBio Co., Ltd. (Guangzhou, China).

RT-qPCR

A TRIzol extraction kit (Invitrogen) was used to extract overall RNA from tissues and cells. Primers were designed and synthesized by Takara (Kyoto, Japan) [Table 1]. Then,

Table 1: Primer sequences for reverse transcription quantitative polymerase chain reaction.

Gene	Primer sequence
miR-26a-5p	F: 5′-ACACTCCAGCTGGGTTCAAGTAATCCAGGA-3′
	R: 5′-TGGTGTCGTGGAGTCG-3′
U6	F: 5′-CTCGCTTCGGCAGCACA-3′
	R: 5′-ACGCTTCACGAATTTGCGT-3′
FUBP1	F: 5′-TAGCAAGGCAGGATTAGTC-3′
	R: 5′-CACGAATTAACTCTAACACCAT-3′
SNHG6	F: 5′-CCTACTGACAACATCGACGTTGAAG-3′
	R: 5′-GGAGAAAACGCTTAGCCATACAG-3′
GAPDH	F: 5′-GGTGGTCTCCTCTGACTTCAACA-3′
	R: 5′-GTTGCTGTAGCCAAATTCGTTGT-3′

F: Forward; *FUBP1*: Far upstream element binding protein 1; *GAPDH*: Glyceraldehyde-3-phosphate dehydrogenase; *miR-26a-5p*: microRNA-26a-5p; R: Reverse; *SNHG6*: Small nucleolar RNA host gene 6.

using the Rever Tra Ace qPCR RT Master Mix kit (TOYOBO, Osaka, Japan), RNA was reverse transcribed into complementary DNA. As instructed by the SYBR® Premix Ex Taq™ II kit (Takara, Dalian, Liaoning, China), quantitative fluorescence PCR was performed in the ABI PRISM® 7300 system (ABI, Inc., Foster City, CA, USA). U6 served as an internal reference for *miR-26a-5p,* while glyceraldehyde-3-phosphate dehydrogenase served as an internal reference for *FUBP1* and *SNHG6*, with the relative expression measured using the $2^{-\Delta\Delta Ct}$ method.

Western blotting analysis

Proteins were extracted from tissues and cells, and the protein concentration of each sample was determined. The 10% sodium dodecyl sulfate (Solarbio) separating and concentrating gels were prepared. The samples were mixed with the loading buffer and boiled for 5 min at 100°C. After an ice bath and centrifugation, equal amounts of sample were added into the lanes with a pipette for electrophoresis separation. Then, proteins in the gel were transferred to cellulose nitrate membranes and blocked with 5% skimmed milk powder at 4°C overnight. Afterward, the membranes were incubated with primary antibodies (Abcam, Cambridge, UK) against *FUBP1* (ab181111, 1:2000), E-cadherin (ab40772, 1:10,000), N-cadherin (ab18203, 1 μg/mL), β-catenin (ab32572, 1:10,000), and Vimentin (ab92547, 1:1000), at 4°C overnight. After that, the membranes were washed with phosphate-buffered saline (PBS, Wuhan Servicebio Co., Ltd., Wuhan, Hubei, China) at room temperature three times for 5 min each time. Subsequently, the membranes were incubated with horseradish peroxidase-labeled secondary antibody immunoglobulin G (1:1000, Boster Biological Technology Co., Ltd, Wuhan, Hubei, China) for 1 h at 37°C, followed by three PBS washes for 5 min each time. The membranes were submerged in enhanced chemiluminescence reaction solution (Pierce Company, now part of Thermo Fisher Scientific, Waltham, MA, USA) at room temperature for 1 min. After liquid removal, the membranes were covered with food preservation film and exposed. After developing and fixing, the images were observed. The protein marker was purchased from Pierce (#84785, Thermo Fisher Scientific) with β-actin as an internal control, and the protein band images were analyzed using ImageJ2x V2.1.4.7 (Rawak Software, Inc., Germany).

Cell counting kit-8 (CCK-8) assay

A PC cell suspension was diluted to a certain concentration and then seeded at a density of 2×10^3 cells/100 mL per well into 96-well plates. Each group had 12 parallel wells. PC cells were cultured for different durations (12, 24, 48, and 72 h, retrospectively), and three replicates were arranged for each time point. CCK-8 solution (Sigma-Aldrich, Merck KGaA, Darmstadt, Germany) was added to the cell-free medium as the blank control. The cells were cultured at 37°C with 5% CO_2. At each time point, 10 μL CCK-8 solution was added to the corresponding wells and incubated in an incubator for 4 h. Finally, the optical density value at 450 nm was measured using a microplate reader and recorded as A_{450nm}.

Colony formation assay

PC cells were detached using trypsin (Solarbio) to fully disperse the suspension in each group. Then, 200 cells were seeded into six-well plates, which were shaken gently to evenly disperse the cells. The cells were cultured for 2 to 3 weeks. When cell colonies were visible to the naked eye, the culture was terminated, and the culture medium was discarded followed by PBS (Wuhan Servicebio) washing. After that, the cells were fixed for 30 min in 4% paraformaldehyde (Solarbio) and washed in PBS three times. Then, the cells were stained in Giemsa staining solution (Shanghai Regal Biology Technology Co, Ltd, Shanghai, China) for 60 min, washed under running water, and air-dried. The plates were inverted and covered with transparent film with a grid. After images were acquired with a Sony HX350 camera (Japan), the cell colony number was directly counted using the naked eye.

Flow cytometry

The staining was carried out according to the instructions of the Annexin V-fluorescein isothiocyanate (FITC)/propidium iodide (PI) kit (BestBio, Shanghai, China). The cells were centrifuged after detachment to remove the supernatant. The cells were resuspended in PBS to adjust the concentration to 1×10^6 cells/mL. Then, 200 μL cells were washed twice using 1 mL pre-cooled PBS followed by centrifugation. The cells were mixed with 2 μL Annexin-V-FITC (20 μg/mL) after being resuspended in 100 μL binding buffer and were incubated on ice, avoiding light exposure, for 15 min. Subsequently, the cells were transferred to a flow cytometry tube, and 300 μL PBS was added. Each sample was mixed with 1 μL PI (50 μg/mL) and detected on a flow cytometer within 30 min.

Hoechst 33258 staining

PC cells (1×10^5 cells/mL) in the logarithmic phase were seeded into six-well plates (3 mL per well) with cover glasses. The cells were incubated (37°C, 5% CO_2) for 24 h, and then the culture solution was discarded. Then, the cells were fixed with fixation solution for 10 min and stained with Hoechst 33258 dye solution (Beyotime Biotechnology Co., Ltd., Shanghai, China) for 5 min away from light at room temperature. The slides with cells attached were placed on the anti-fluorescence quencher droplets. A fluorescence microscope (BX60, Olympus Optical Co., Ltd, Tokyo, Japan) was used to observe the slides, and images were collected.

Transwell assay

When PC cells reached the logarithmic phase, they were cultured at 37°C for 24 h in six-well plates before transfection. After 48 h of culture, 0.25% trypsin was added to the cells, and the cells were resuspended in DMEM to adjust the concentration to 5×10^5 cells/mL. The basolateral chamber was filled with 500 μL DMEM containing 10% FBS (Solarbio), while the apical chamber was filled with 200 μL cell suspension followed by 24 h incubation at 37°C. The chambers were transferred to a clean 24-well plate, and 4% polyformaldehyde (500 μL,

Solarbio) was added to each well. The cells were fixed for 30 min at room temperature, stained with crystal violet (Solarbio) for 60 min, and washed with PBS (Servicebio) two or three times. Five images were collected from each well and analyzed.

The invasion chamber was coated with 50 μL Matrigel at 500 g/μL (Becton, Dickinson and Company, Franklin Lakes, NJ, USA). The Matrigel was solidified at 37°C for 4 h. The next steps were similar to those in the cell migration experiment mentioned above.

Dual luciferase reporter gene assay

Bioinformatics software (http://starbase.sysu.edu.cn/panGeneDiffExp.php) was used to predict the target relationship between *miR-26a-5p* and *SNHG6* as well as the binding site. The *SNHG6* sequence containing the binding site of *miR-26a-5p* was synthesized and inserted into the pMIR-REPORT™ Luciferase vector (Ambion, Austin, TX, USA) to construct the *SNHG6* wild-type plasmid (*SNHG6*-WT). In this plasmid, the binding site was mutated to construct the *SNHG6* mutant plasmid (*SNHG6*-MUT). Plasmid extraction was carried out according to the instructions of the plasmid extraction kit (Promega, Madison, Wisconsin, USA). *SNHG6*-WT and *SNHG6*-MUT were mixed with mimic NC and *miR-26a-5p* mimic (Shanghai GenePharma Biological Co., Ltd., Shanghai, China), respectively, followed by co-transfection into 293T cells, which were obtained from ATCC, using Lipofectamine™ 2000. Luciferase activity was measured by a luciferase detection kit and a GloMax 20/20luminometer (Promega). As described above, the target relationship between *miR-26a-5p* and *FUBP1* as well as the binding site was predicted by http://www.targetscan.org, and the plasmids *FUBP1*-WT and *FUBP1*-MUT were constructed.

RNA pull-down assay

The experimental procedure was carried out according to the instructions of the biotin RNA labeling mix kit (Roche Diagnostics, Indianapolis, IN, USA). The biotin-labeled *miR-26a-5p* WT and *miR-26a-5p* MUT were incubated with MIAPaCa-2 cytoplasmic extract. Cells were resuspended in lysis buffer, placed on ice for 10 min, and centrifuged for 10 min at 10,000 × g. The magnetic beads coated with streptavidin (Thermo Fisher Scientific) were blocked with lysis buffer containing yeast tRNA and bovine serum albumin at 4°C for 2 h and washed twice with 1 mL lysis buffer. The lysate was added to the magnetic beads coated with streptavidin and incubated at 4°C for 4 h. Then, the cells were washed twice with 1 mL lysis buffer, three times with low salt buffer, and one time with high salt buffer. RNA bound to magnetic beads was separated by TRIzol reagent (Thermo Fisher Scientific). *SNHG6* expression was detected by RT-qPCR.

Xenograft tumor model in nude mice

si-NC or si-*SNHG6*-1 was used to treat nude mice (five mice in each group, 6 weeks old) (Cancer Research Institute of Chinese Academy of Medical Sciences, Beijing, China). Panc-1 cells that were stably growing in the logarithmic phase were collected and resuspended in PBS, the supernatant was then removed, and the cell concentration was adjusted to 1×10^7 cells/mL. Each nude mouse was injected subcutaneously with 200 μL cell suspension via the right hind leg and housed under the same conditions for 4 weeks. Tumor volume was measured with Vernier calipers once every 7 days. After 28 days, nude mice were killed by cervical dislocation, and the tumors were weighed. The obtained tumors were made into tissue homogenate. The levels of *SNHG6*, *miR-26a-5p*, and *FUBP1* were detected by RT-qPCR and western blotting analysis.

Statistical analysis

SPSS21.0 (IBM, Armonk, NY, USA) was used for data analysis. The Kolmogorov-Smirnov test was performed to test whether the data were normally distributed. Data are expressed as the mean ± standard deviation. The *t* test was conducted for comparisons between two groups. One-way or two-way analysis of variance was performed to compare data among multiple groups, followed by Tukey multiple comparison test. The *P* value was calculated by a bilateral test, and $P < 0.05$ indicated a statistically significant difference.

Results

SNHG6 was upregulated in PC

SNHG6 expression was predicted by bioinformatics analysis and verified by RT-qPCR. Through the http://starbase.sysu.edu.cn/panGeneDiffExp.php website, we found that *SNHG6* was overexpressed in PC tissues compared to adjacent normal tissues in 178 PC patients [Figure 1A]. To verify the results, five pairs of PC and adjacent normal tissues were tested by RT-qPCR. The results were consistent with the database results [Figure 1B]. The RT-qPCR data also showed that among four PC cell lines (MIAPaCa-2, BxPC-3, Capan-1, and Panc-1), *SNHG6* expression was the highest in Panc-1 cells, followed by Capan-1 cells and BxPC-3 cells, with the lowest expression in MIAPaCa-2 cells ($P < 0.01$) [Figure 1C].

Silencing SNHG6 promoted apoptosis but inhibited the proliferation, invasion, and migration of PC cells

Next, the changes in PC cell biology were surveyed after transfection of the Panc-1 cell line with si-*SNHG6*. si-*SNHG6* decreased *SNHG6* expression in Panc-1 cells [Figure 2A], downregulated β-catenin, Vimentin, and N-cadherin levels, upregulated E-cadherin levels [Figure 2B], inhibited cell proliferation in a time-dependent manner [Figure 2C], reduced the cell colony formation rate [Figure 2D], accelerated cell apoptosis [Figure 2E], induced highly aggregated nuclear chromatin and nuclear rupture [Figure 2F], and inhibited cell migration and invasion [Figure 2G]. The MIAPaCa-2 cell line treated with a plasmid overexpressing *SNHG6* showed the opposite results.

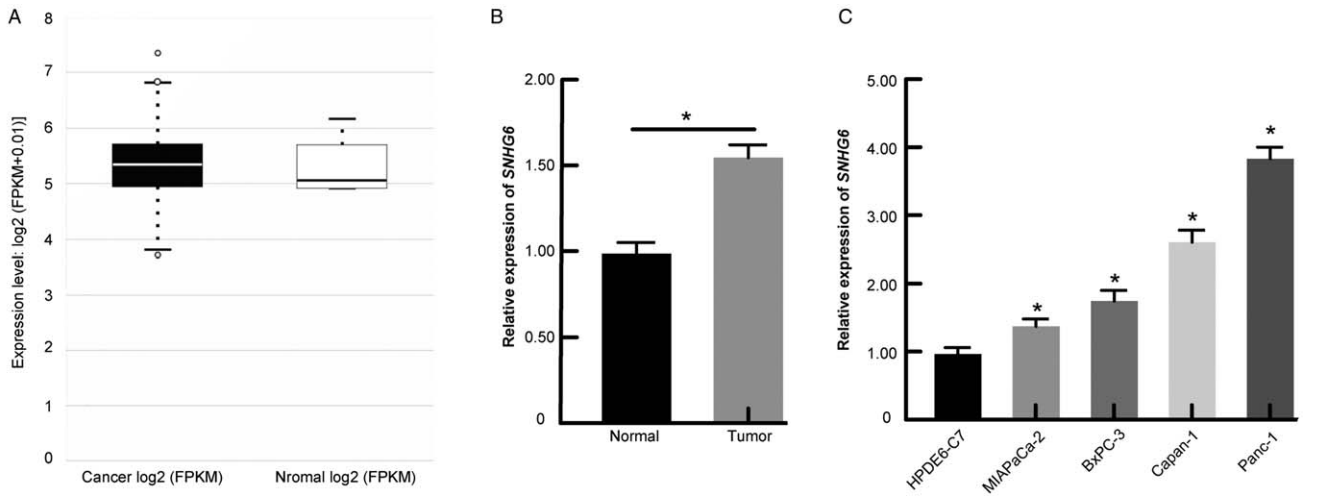

Figure 1: *SNHG6* was overexpressed in PC. (A) The different expression of *SNHG6* in PC tissues and adjacent normal tissues was obtained from the StarBase online database, and *SNHG6* expression in PC tissues was upregulated; (B–C) *SNHG6* expression in tumor tissues, adjacent normal tissues, four PC cell lines (MIAPaCa-2, BxPC-3, Capan-1, and Panc-1) and a human normal pancreatic ductal epithelial cell line (HPDE6-C7) was detected using RT-qPCR and western blot analysis, and the results showed that *SNHG6* expression in PC tissues and cell lines was upregulated. In panel B, a *t* test was performed for data analysis; $^{*}P < 0.01$ *vs.* the adjacent normal tissues; $n = 5$. In panel C, one-way ANOVA and Tukey multiple comparisons test were used. $^{*}P < 0.01$ *vs.* HPDE6-C7 cells, $n = 3$. ANOVA: Analysis of variance; FPKM: Fragments per kilobase million; PC: Pancreatic cancer; RT-qPCR: Reverse transcription quantitative polymerase chain reaction; *SNHG6*: Small nucleolar RNA host gene 6.

SNHG6 upregulated FUBP1 by sponging miR-26a-5p

Subsequently, the relationships among *SNHG6*, *miR-26a-5p* and *FUBP1* were characterized. Through online analysis, we found a specific binding site between the sequences of *SNHG6* and *miR-26a-5p* [Figure 3A]. In the Panc-1 cell line treated with si-*SNHG6*, *miR-26a-5p* was upregulated, while in the MIAPaCa-2 cell line overexpressing *SNHG6*, *miR-26a-5p* was downregulated (both $P < 0.01$) [Figure 3B]. The relative luciferase activity of *miR-26a-5p* in the *SNHG6* WT plasmid-transfected cells was decreased, as detected by a dual luciferase reporter gene assay ($P < 0.01$) [Figure 3C]. The RNA pull-down assay showed that *miR-26a-5p* could pull down *SNHG6* ($P < 0.01$) [Figure 3D].

Through online analysis, we found a specific binding site between sequences of the *FUBP1* gene and the *miR-26a-5p* sequence [Figure 3E]. *FUBP1* was downregulated in the MIAPaCa-2 cell line overexpressing *miR-26a-5p* ($P < 0.01$) [Figure 3F and G]. The luciferase activity of the *miR-26a-5p* mimic in the *FUBP1* 3′UTR WT plasmid was decreased ($P < 0.01$) [Figure 3H]. A dual luciferase reporter gene assay validated the targeting binding of *miR-26a-5p* to *FUBP1*. *FUBP1* was downregulated in the Panc-1 cell line treated with si-*SNHG6* ($P < 0.01$) [Figure 3I–J].

Overexpressed miR-26a-5p abolished the effect of overexpressed SNHG6 on PC cells

Compared with MIAPaCa-2 cells overexpressing *miR-26a-5p*, the MIAPaCa-2 cell line treated with the *SNHG6* overexpression plasmid and mimic NC showed decreased *miR-26a-5p* expression [Figure 4A], increased cell proliferation [Figure 4B], a higher cell colony formation rate [Figure 4C], reduced cell apoptosis [Figure 4D and 4E], and increased cell migration and invasion (all $P < 0.01$) [Figure 4F]. However, when the *miR-26a-5p* mimic was transfected into MIAPaCa-2 cells treated with the *SNHG6* overexpression plasmid, it was found that overexpression of *miR-26a-5p* inhibited the growth and metastasis of MIAPaCa-2 cells with *SNHG6* upregulation compared with the mimic NC transfection.

Silencing SNHG6 inhibited tumor formation in nude mice

After silencing *SNHG6*, the expression of *FUBP1* and *SNHG6* in tumor tissues was significantly decreased, while *miR-26a-5p* expression was increased (all $p < 0.01$) [Figure 5A and 5B], and the growth rate and weight of tumors in nude mice were reduced when compared with those in nude mice treated with si-NC [Figure 5C and 5E], which further confirmed that *SNHG6* promoted tumor growth.

Discussion

PC is related to a poor prognosis, evidenced by the close link between disease occurrence and mortality.[21] LncRNAs have been indicated to be modulators of cellular development and human diseases via their effects on gene expression.[22] They are also competing endogenous RNAs that regulate miRs and the expression of their target genes, thus influencing cancer development.[23] Herein, we discussed the underlying mechanisms of *SNHG6*, *FUBP1*, and *miR-26a-5p* in PC progression. The evidence obtained from both PC tissues and cell lines demonstrated that silencing *SNHG6* could ameliorate PC by sponging *miR-26a-5p*.

Initially, *SNHG6* was overexpressed in PC tissues, and silencing *SNHG6* inhibited epithelial-mesenchymal transition (EMT) and ameliorated cell activities in PC. LncRNA *SNHG6*, a recently identified cancer-related lncRNA, was found to be upregulated in Wilms' tumor.[24] Another study proved that *SNHG6* was upregulated in ovarian

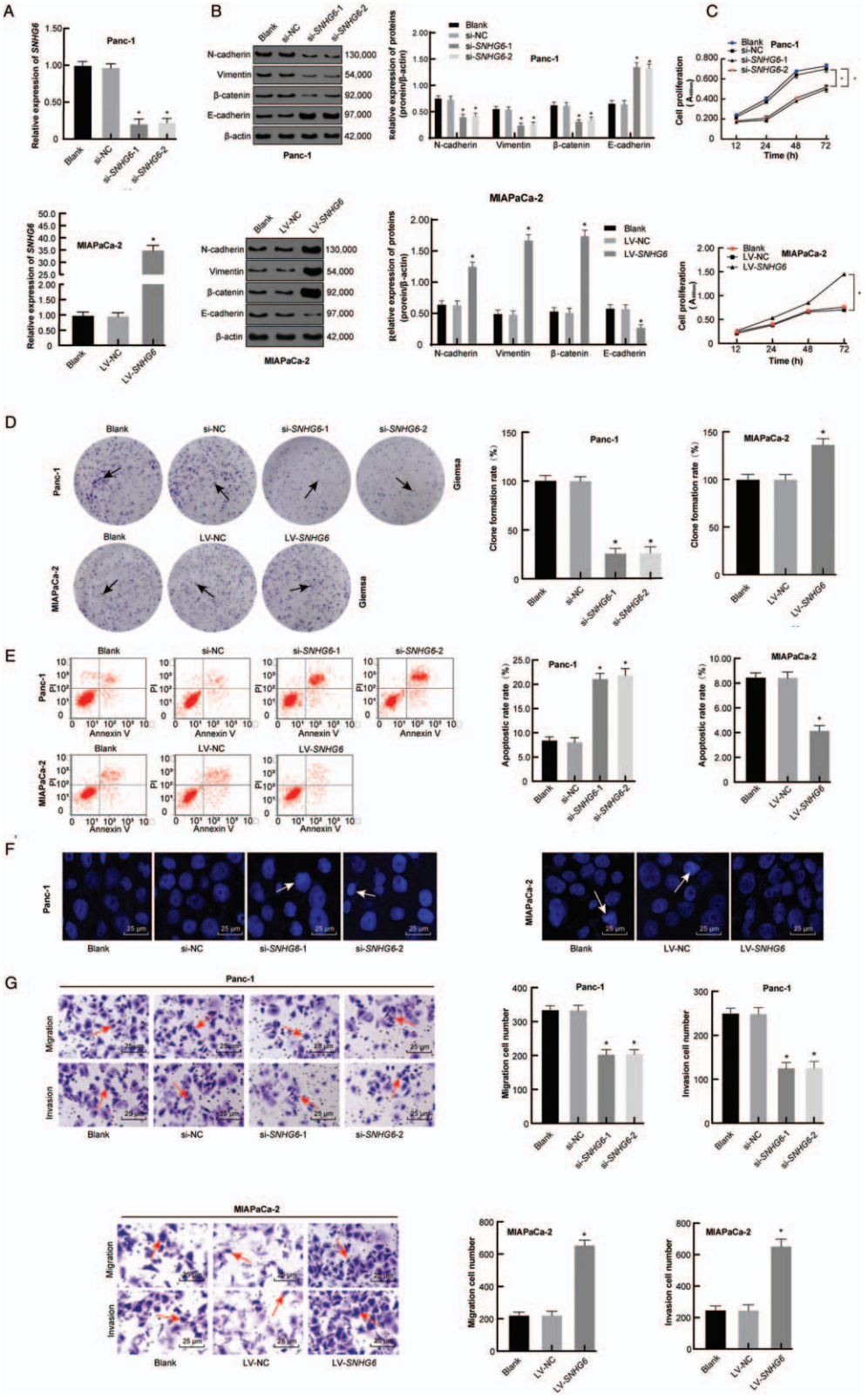

Figure 2: Cell aggressiveness was inhibited, while cell apoptosis was increased after downregulating *SNHG6*. (A) *SNHG6* expression in the Panc-1 cell line treated with si-*SNHG6* and the MIAPaCa-2 cell line overexpressing *SNHG6* detected by RT-qPCR; (B) expression of EMT-related proteins in the Panc-1 cell line treated with si-*SNHG6* and in the MIAPaCa-2 cell line overexpressing *SNHG6* detected by western blotting analysis; (C and D) proliferation of Panc-1 cells treated with si-*SNHG6* and MIAPaCa-2 cells overexpressing *SNHG6* determined by colony formation and CCK-8 assays; the black arrow indicates a cell colony; (E and F) apoptosis of Panc-1 cells treated with si-*SNHG6* and MIAPaCa-2 cells overexpressing *SNHG6* detected by Hoechst 33258 staining and flow cytometry; the bright blue cells indicated by the white arrows are apoptotic cells, ×200; (G) migration and invasion of Panc-1 cells treated with si-*SNHG6* and MIAPaCa-2 cells overexpressing *SNHG6* detected by Transwell assay; the red arrow indicates migrated and invasive cells, ×400. One-way ANOVA was used in panels A, D, E, and G, while two-way ANOVA was used in panels B and C, followed by Tukey multiple comparisons test. $^{*}P < 0.01$ *vs.* the LV-NC group, $n = 3$. ANOVA: Analysis of variance; CCK-8: Cell counting kit-8; EMT: Epithelial mesenchymal transition; LV-NC: pCD513B-1; LV-*SNHG6*: pCD513B-1-*SNHG6*; OD: Optical density; RT-qPCR: Reverse transcription quantitative polymerase chain reaction; si-NC: Small interfering RNA negative control; *SNHG6*: Small nucleolar RNA host gene 6; si-SNHG6: Small interfering RNA-*SNHG6*.

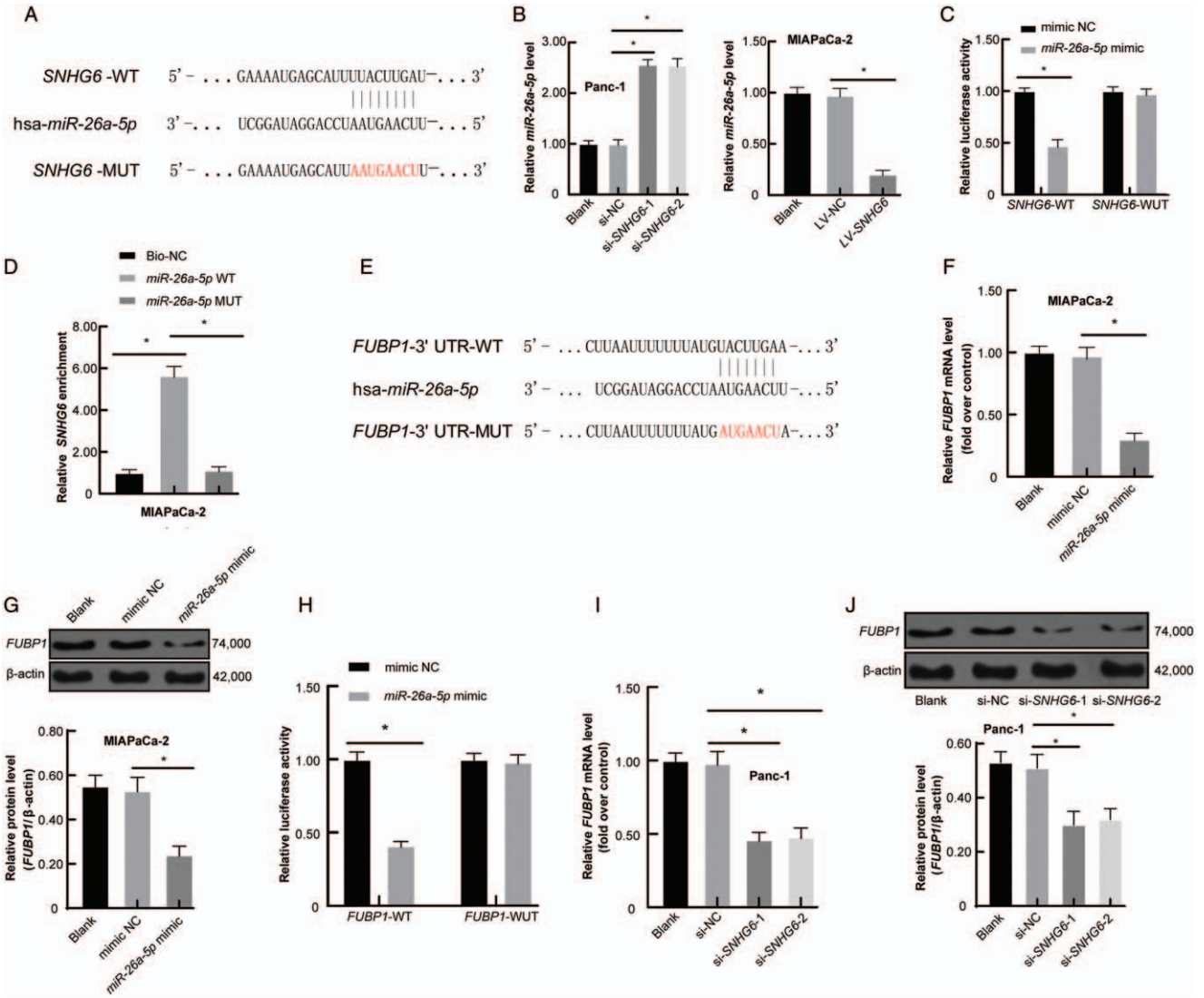

Figure 3: *SNHG6* inhibited *miR-26a-5p* expression to upregulate *FUBP1* expression. (A) Prediction of binding sites between the *SNHG6* sequence and *miR-26a-5p* sequence by the StarBase online database; (B) *miR-26a-5p* expression in the Panc-1 cell line treated with si-*SNHG6* and in the MIAPaCa-2 cell line overexpressing *SNHG6* detected by RT-qPCR; (C) the relationship between *SNHG6* and *miR-26a-5p* verified by dual luciferase reporter gene assay; (D) RNA pull-down between *SNHG6* and *miR-26a-5p*, and expression in MIAPaCa-2 cells was detected by RT-qPCR, which showed that *SNHG6* expression in the *miR-26a-5p* NC group was decreased; (E) prediction of the binding sites between the *FUBP1* sequence and *miR-26a-5p* sequence by the TargetScan online database; (F and G) *FUBP1* expression in the MIAPaCa-2 cell line overexpressing *miR-26a-5p* detected by RT-qPCR and western blot analysis; (H) the relationship between *FUBP1* and *miR-26a-5p* verified by dual luciferase reporter gene assay; (I and J) *FUBP1* expression in the Panc-1 cell line treated with si-*SNHG6* detected by RT-qPCR and western blot analysis. One-way ANOVA was used in panels B, D, F, G, I, and J, and two-way ANOVA was used in panels C and H, followed by Tukey multiple comparisons test. $^{*}P < 0.01$. $n = 3$. ANOVA: Analysis of variance; *FUBP1*: Far upstream element binding protein1; *miR-26a-5p*: MicroRNA-26a-5p; mimic NC: Mimic negative control; MUT: Mutant; RT-qPCR: Reverse transcription quantitative polymerase chain reaction; si-NC: Small interfering RNA negative control; *SNHG6*: Small nucleolar RNA host gene 6; si-SNHG6: Small interfering RNA-*SNHG6*; WT: Wild type.

clear cell carcinoma and that upregulated *SNHG6* contributed to the tumorigenesis and progression of ovarian clear cell carcinoma.[25] Zhang *et al*[26] found that knockdown of *SNHG6* inhibited colorectal cancer cell activities and EMT by regulating *EZH2* expression by sponging *miR-26a*. Similar to our study, *SNHG6* was reported by Yan *et al*[10] to be overexpressed in PC, which predicted poor prognosis as well.

Our present study also implied that *SNHG6* upregulated *FUBP1* by sponging *miR-26a-5p*. In osteosarcoma cells, *SNHG6* competitively binds to *miR-26a-5p*, and *SNHG6* acts as an oncogene by regulating *miR-26a-5p*/unc-51-like autophagy activating kinase (*ULK1*) at the post-transcriptional level.[11] In breast cancer, *SNHG6* acts as a ceRNA by negatively regulating *miR-26a-5p*.[16] In human lung adenocarcinoma, *SNHG6* competitively binds to *miR-26a-5p* and controls *E2F7* expression to promote cell motility and EMT.[15] All this evidence confirmed the relationship between *SNHG6* and *miR-26a-5p* in different types of diseases. Sun *et al*[27] stated that *SNHG1* promoted tumor growth via inhibition of *FUBP1* and binding to FBP-interacting repressor (FIR), therefore repressing *FIR*-mediated MYC transcriptional inhibition. Another study suggested that *FUBP1* was the target gene of *miR-16-1* and that *miR-16-1* could inhibit *FUBP1* directly and specifically in gastric cancer.[28] A study also identified *FUBP1* as a novel *miR-16* target, and *miR-16* overexpression decreased *FUBP1* levels in human breast cancer and gastric cancer cells.[29]

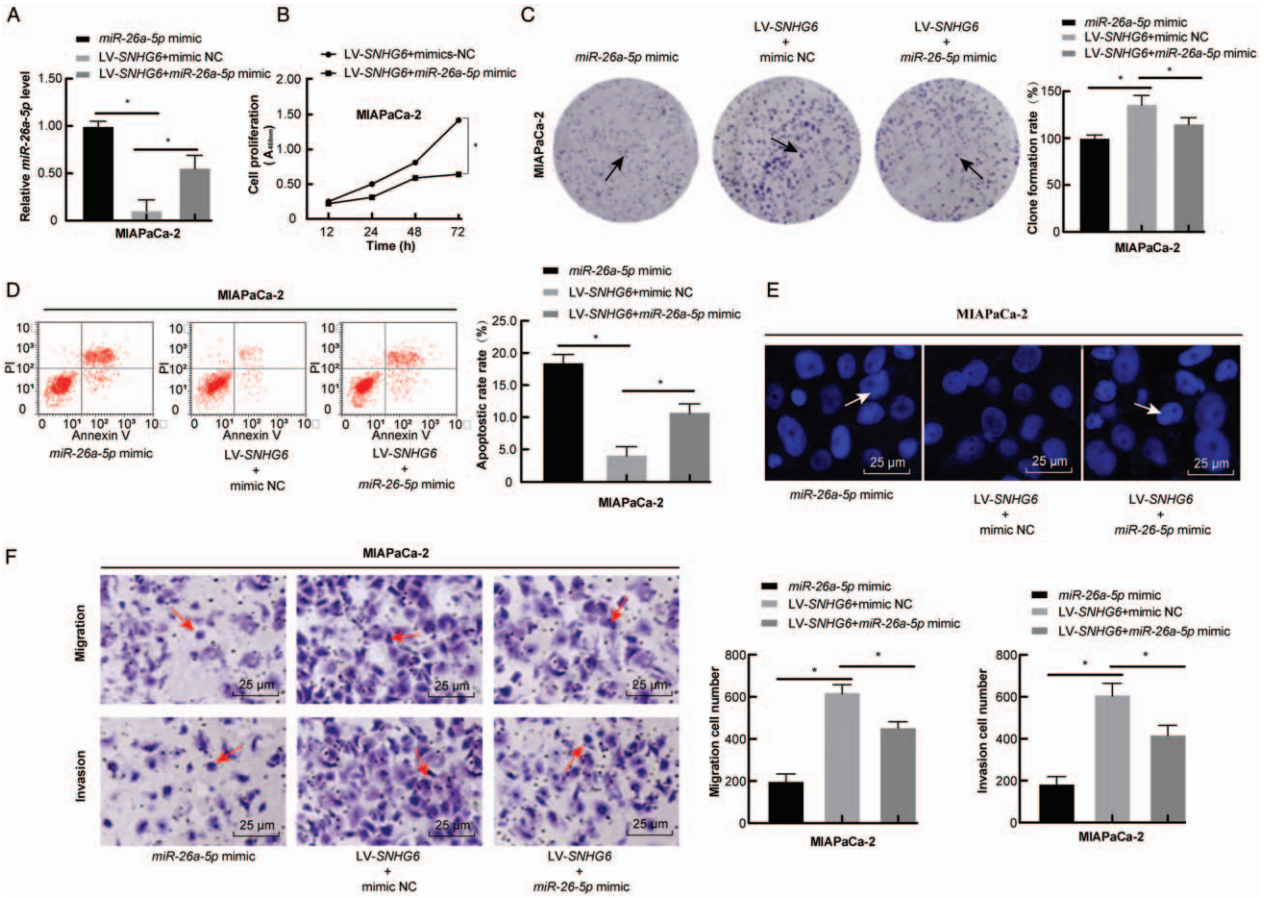

Figure 4: The effects of *SNHG6* overexpression on PC cells were blocked by *miR-26a-5*p overexpression. (A) *miR-26a-5p* expression in the MIAPaCa-2 cell line treated with overexpressed *SNHG6* and *miR-26a-5p* mimic detected by RT-qPCR; (B and C) cell proliferation in MIAPaCa-2 cell line treated with the *SNHG6* overexpression plasmid and *miR-26a-5p* mimic detected by CCK-8 assay and colony formation assay; the black arrow indicates a cell colony; (D and E) cell apoptosis detected by flow cytometry and Hoechst 33258 staining; the white arrow indicates apoptotic cells, ×200; (F) cell migration and invasion detected by Transwell assay; the red arrow indicates migrated and invasive cells, ×400. Data in panel B were analyzed using two-way ANOVA, and data in the other panels were analyzed using one-way ANOVA, followed by Tukey multiple comparisons test; $^{*}P < 0.01$; $n = 3$. ANOVA: Analysis of variance; CCK-8: Cell counting kit-8; LV-NC: pCD513B-1; LV-*SNHG6*: pCD513B-1-*SNHG6*; mimic NC: Mimic negative control; *miR-26a-5*: microRNA-26a-5; OD: Optical density; RT-qPCR: Reverse transcription quantitative polymerase chain reaction; *SNHG6*: Small nucleolar RNA host gene 6.

Furthermore, we also concluded that overexpressed *miR-26a-5p* inhibited EMT in PC. *miR-26a-5p* was found to block cell migration in assorted malignant tumors. For instance, *miR-26a-5p* was indicated to be downregulated in malignant melanoma, and forced expression of *miR-26a* blocked melanoma cell invasiveness and growth through mediation of microphthalmia-associated transcription factors.[30] An obvious downregulation of *miR-26a-5p* was also observed in bladder cancer and hepatocellular carcinoma, and downregulated *miR-26a-5p* accelerated cell invasion, migration, and EMT processes.[31,32] One study discovered that *SNHG5* triggered melanoma cell aggressiveness while hindering apoptosis by sponging *miR-26a-5p*.[33] *FUBP1* was found to be involved in the regulation of diverse cellular actions and correlated with oncogenesis.[34] Upregulated *FUBP1* was observed, and *FUBP1* was suggested to be an indicator and a possible target in sacral chordomas and human clear cell renal cell carcinoma.[35,36] A recent study elucidated that *FUBP1* was an important transactivator of the c-Myc proto-oncogene overexpressed in PC and inhibited cancer cell activities by increasing *PD-L1* expression modulated by Myc.[37] We found that overexpressed *miR-26a-5p* could inhibit the expression of FUBP1, thereby ameliorating PC progression.

Consistent with previous studies, we confirmed that *SNHG6* is an oncogenic lncRNA in PC. Through our investigation *in vitro* and *in vivo*, we proved that *SNHG6* could accelerate PC cell activities by regulating *FUBP1* to a higher level by sponging *miR-26a-5p*. Furthermore, our study revealed encouraging data that suggest the value of *miR-26a-5p* as a tumor inhibitor and a potential target for PC. In the future, we will investigate and discuss the potential mechanism of the *miR-26a-5p* target gene *FUBP1* and deeply estimate the underlying effects of other miRs regulated by *SNHG6* in PC progression. Further studies on tissues from PC patients are required to fully understand the detailed mechanisms of *SNHG6*, *miR-26a-5p*, and *FUBP1* in PC.

Funding

This study was supported by a grant from the Shanghai University of Medicine & Health Sciences Seed Foundation (No. SFP-18-22-15-002).

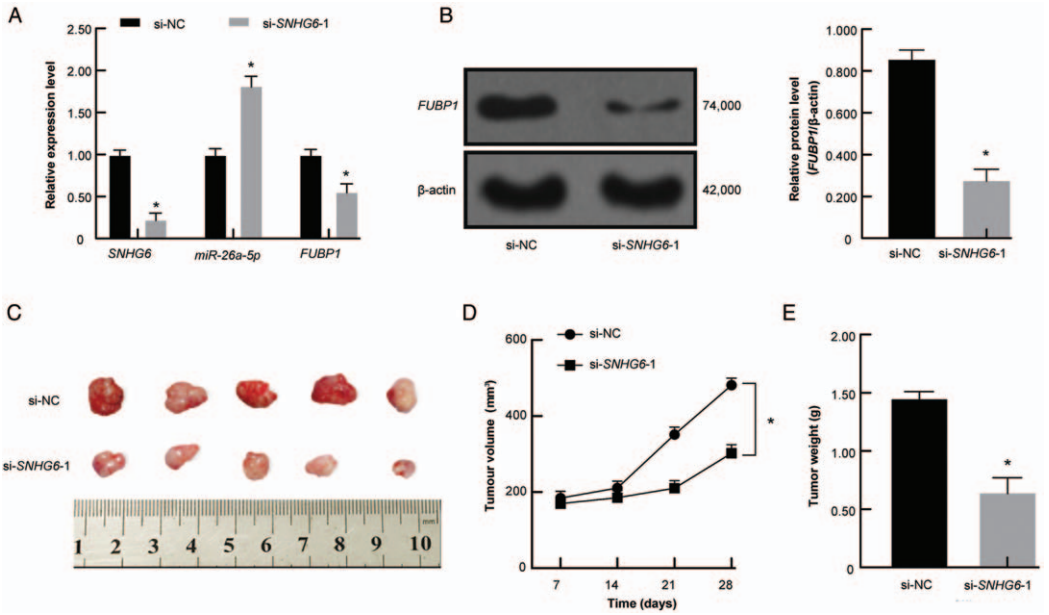

Figure 5: Tumor formations in nude mice was blocked by silencing *SNHG6*. (A) Expression of *SNHG6*, *FUBP1*, and *miR-26a-5p* in tumors detected by RT-qPCR after inhibition of *SNHG6* expression; (B) expression of *FUBP1* in tumors detected by western blot analysis after inhibition of *SNHG6* expression; (C–E) tumor images at the 28th day, tumor volume and weight in nude mice treated with si-NC or si-*SNHG6*-1 within 28 days. Two-way ANOVA was used in panels A and D followed by Tukey multiple comparisons test, and the *t*-test was used in panels B and E. $^{*}P < 0.01$ *vs.* the si-NC group, $n = 5$. ANOVA: Analysis of variance; *FUBP1*: Far upstream element binding protein1; *miR-26a-5*: microRNA-26a-5; si-NC: Small interfering RNA negative control; si-SNHG6-1: Small interfering RNA-small nucleolar RNA host gene 6-1; *SNHG6*: Small nucleolar RNA host gene 6.

Conflicts of interest

None.

References

1. Yang Y, Sun Y, Wang H, Li H, Zhang M, Zhou L, *et al*. MicroRNA-221 induces autophagy through suppressing HDAC6 expression and promoting apoptosis in pancreatic cancer. Oncol Lett 2018;16:7295–7301. doi: 10.3892/ol.2018.9513.
2. Zhang JJ, Jia JP, Shao Q, Wang YK. Diabetes mellitus and risk of pancreatic cancer in China: a meta-analysis based on 26 case-control studies. Prim Care Diabetes 2019;13:276–282. doi: 10.1016/j.pcd.2018.11.015.
3. Biankin AV, Waddell N, Kassahn KS, Gingras MC, Muthuswamy LB, Johns AL, *et al*. Pancreatic cancer genomes reveal aberrations in axon guidance pathway genes. Nature 2012;491:399–405. doi: 10.1038/nature11547.
4. Costello E, Neoptolemos JP. Pancreatic cancer in 2010: new insights for early intervention and detection. Nat Rev Gastroenterol Hepatol 2011;8:71–73. doi: 10.1038/nrgastro.2010.214.
5. Ali S, Saleh H, Sethi S, Sarkar FH, Philip PA. MicroRNA profiling of diagnostic needle aspirates from patients with pancreatic cancer. Br J Cancer 2012;107:1354–1360. doi: 10.1038/bjc.2012.383.
6. Yan X, Hu Z, Feng Y, Hu X, Yuan J, Zhao SD, *et al*. Comprehensive genomic characterization of long non-coding RNAs across human cancers. Cancer Cell 2015;28:529–540. doi: 10.1016/j.ccell.2015.09.006.
7. Zhang X, Liu Z, Shu Q, Yuan S, Xing Z, Song J. LncRNA SNHG6 functions as a ceRNA to regulate neuronal cell apoptosis by modulating miR-181c-5p/BIM signalling in ischaemic stroke. J Cell Mol Med 2019;23:6120–6130. doi: 10.1111/jcmm.14480.
8. Li K, Ma YB, Tian YH, Xu XL, Gao Y, He YQ, *et al*. Silencing lncRNA SNHG6 suppresses proliferation and invasion of breast cancer cells through miR-26a/VASP axis. Pathol Res Pract 2019;215:152575. doi: 10.1016/j.prp.2019.152575.
9. Meng S, Jian Z, Yan X, Li J, Zhang R. LncRNA SNHG6 inhibits cell proliferation and metastasis by targeting ETS1 via the PI3K/AKT/mTOR pathway in colorectal cancer. Mol Med Rep 2019;20:2541–2548. doi: 10.3892/mmr.2019.10510.
10. Yan Y, Chen Z, Xiao Y, Wang X, Qian K. Long non-coding RNA SNHG6 is upregulated in prostate cancer and predicts poor prognosis. Mol Biol Rep 2019;46:2771–2778. doi: 10.1007/s11033-019-04723-9.
11. Zhu X, Yang G, Xu J, Zhang C. Silencing of SNHG6 induced cell autophagy by targeting miR-26a-5p/ULK1 signaling pathway in human osteosarcoma. Cancer Cell Int 2019;19:82. doi: 10.1186/s12935-019-0794-1.
12. Song W, Li Q, Wang L, Wang L. Modulation of FoxO1 expression by miR-21 to promote growth of pancreatic ductal adenocarcinoma. Cell Physiol Biochem 2015;35:184–190. doi: 10.1159/000369686.
13. Huang ZM, Ge HF, Yang CC, Cai Y, Chen Z, Tian WZ, *et al*. MicroRNA-26a-5p inhibits breast cancer cell growth by suppressing RNF6 expression. Kaohsiung J Med Sci 2019;35:467–473. doi: 10.1002/kjm2.12085.
14. Shi D, Wang H, Ding M, Yang M, Li C, Yang W, *et al*. MicroRNA-26a-5p inhibits proliferation, invasion and metastasis by repressing the expression of Wnt5a in papillary thyroid carcinoma. Onco Targets Ther 2019;12:6605–6616. doi: 10.2147/OTT.S205994.
15. Liang R, Xiao G, Wang M, Li X, Li Y, Hui Z, *et al*. SNHG6 functions as a competing endogenous RNA to regulate E2F7 expression by sponging miR-26a-5p in lung adenocarcinoma. Biomed Pharmacother 2018;107:1434–1446. doi: 10.1016/j.biopha.2018.08.099.
16. Lv P, Qiu X, Gu Y, Yang X, Xu X, Yang Y. Long non-coding RNA SNHG6 enhances cell proliferation, migration and invasion by regulating miR-26a-5p/MAPK6 in breast cancer. Biomed Pharmacother 2019;110:294–301. doi: 10.1016/j.biopha.2018.11.016.
17. Batchu RB, Gruzdyn OV, Qazi AM, Kaur J, Mahmud EM, Weaver DW, *et al*. Enhanced phosphorylation of p53 by microRNA-26a leading to growth inhibition of pancreatic cancer. Surgery 2015;158:981–986. doi: 10.1016/j.surg.2015.05.019.
18. Deng J, He M, Chen L, Chen C, Zheng J, Cai Z. The loss of miR-26a-mediated post-transcriptional regulation of cyclin E2 in pancreatic cancer cell proliferation and decreased patient survival. PLoS One 2013;8:e76450. doi: 10.1371/journal.pone.0076450.
19. Hoang VT, Verma D, Godavarthy PS, Llavona P, Steiner M, Gerlach K, *et al*. The transcriptional regulator FUBP1 influences disease outcome in murine and human myeloid leukemia. Leukemia 2019;33:1700–1712. doi: 10.1038/s41375-018-0358-8.
20. Yuan YH, Zhou J, Zhang Y, Xu MD, Wu J, Li W, *et al*. Identification of key genes and pathways downstream of the beta-catenin-TCF7L1

complex in pancreatic cancer cells using bioinformatics analysis. Oncol Lett 2019;18:1117–1132. doi: 10.3892/ol.2019.10444.
21. Kamisawa T, Wood LD, Itoi T, Takaori K. Pancreatic cancer. Lancet 2016;388:73–85. doi: 10.1016/S0140-6736(16)00141-0.
22. Assmann TS, Milagro FI, Martinez JA. Crosstalk between microRNAs, the putative target genes and the lncRNA network in metabolic diseases. Mol Med Rep 2019;20:3543–3554. doi: 10.3892/mmr.2019.10595.
23. Li F, Li Q, Wu X. Construction and analysis for differentially expressed long non-coding RNAs and microRNAs mediated competing endogenous RNA network in colon cancer. PLoS One 2018;13:e0192494. doi: 10.1371/journal.pone.0192494.
24. Su L, Wu A, Zhang W, Kong X. Silencing long non-coding RNA SNHG6 restrains proliferation, migration and invasion of Wilms' tumour cell lines by regulating miR-15a. Artif Cells Nanomed Biotechnol 2019;47:2670–2677. doi: 10.1080/21691401.2019.1633338.
25. Wu Y, Deng Y, Guo Q, Zhu J, Cao L, Guo X, *et al*. Long non-coding RNA SNHG6 promotes cell proliferation and migration through sponging miR-4465 in ovarian clear cell carcinoma. J Cell Mol Med 2019;23:5025–5036. doi: 10.1111/jcmm.14359.
26. Zhang M, Duan W, Sun W. LncRNA SNHG6 promotes the migration, invasion, and epithelial-mesenchymal transition of colorectal cancer cells by miR-26a/EZH2 axis. Onco Targets Ther 2019;12:3349–3360. doi: 10.2147/OTT.S197433.
27. Sun Y, Wei G, Luo H, Wu W, Skogerbo G, Luo J, *et al*. The long noncoding RNA SNHG1 promotes tumor growth through regulating transcription of both local and distal genes. Oncogene 2017;36:6774–6783. doi: 10.1038/onc.2017.286.
28. Zhao D, Zhang Y, Song L. MiR-16-1 targeted silences far upstream element binding protein 1 to advance the chemosensitivity to adriamycin in gastric cancer. Pathol Oncol Res 2018;24:483–488. doi: 10.1007/s12253-017-0263-x.
29. Venturutti L, Cordo Russo RI, Rivas MA, Mercogliano MF, Izzo F, Oakley RH, *et al*. MiR-16 mediates trastuzumab and lapatinib response in ErbB-2-positive breast and gastric cancer via its novel targets CCNJ and FUBP1. Oncogene 2016;35:6189–6202. doi: 10.1038/onc.2016.151.
30. Qian H, Yang C, Yang Y. MicroRNA-26a inhibits the growth and invasiveness of malignant melanoma and directly targets on MITF gene. Cell Death Discov 2017;3:17028. doi: 10.1038/cddiscovery.2017.28.
31. Chang L, Li K, Guo T. miR-26a-5p suppresses tumor metastasis by regulating EMT and is associated with prognosis in HCC. Clin Transl Oncol 2017;19:695–703. doi: 10.1007/s12094-016-1582-1.
32. Miyamoto K, Seki N, Matsushita R, Yonemori M, Yoshino H, Nakagawa M, *et al*. Tumour-suppressive miRNA-26a-5p and miR-26b-5p inhibit cell aggressiveness by regulating PLOD2 in bladder cancer. Br J Cancer 2016;115:354–363. doi: 10.1038/bjc.2016.179.
33. Gao J, Zeng K, Liu Y, Gao L, Liu L. LncRNA SNHG5 promotes growth and invasion in melanoma by regulating the miR-26a-5p/TRPC3 pathway. Onco Targets Ther 2019;12:169–179. doi: 10.2147/OTT.S184078.
34. Debaize L, Troadec MB. The master regulator FUBP1: its emerging role in normal cell function and malignant development. Cell Mol Life Sci 2019;76:259–281. doi: 10.1007/s00018-018-2933-6.
35. Duan J, Bao X, Ma X, Zhang Y, Ni D, Wang H, *et al*. Upregulation of far upstream element-binding protein 1 (FUBP1) promotes tumor proliferation and tumorigenesis of clear cell renal cell carcinoma. PLoS One 2017;12:e0169852. doi: 10.1371/journal.pone.0169852.
36. Wen H, Ma H, Li P, Zheng J, Yu Y, Lv G. Expression of far upstream element-binding protein 1 correlates with c-Myc expression in sacral chordomas and is associated with tumor progression and poor prognosis. Biochem Biophys Res Commun 2017;491:1047–1054. doi: 10.1016/j.bbrc.2017.08.008.
37. Fan P, Ma J, Jin X. Far upstream element-binding protein 1 is upregulated in pancreatic cancer and modulates immune response by increasing programmed death ligand 1. Biochem Biophys Res Commun 2018;505:830–836. doi: 10.1016/j.bbrc.2018.10.009.

How to cite this article: Zhang XX, Chen H, Li HY, Chen R, He L, Yang JL, Xiao LL, Chen JL. Long non-coding RNA small nucleolar RNA host gene 6 aggravates pancreatic cancer through upregulation of far upstream element binding protein 1 by sponging microRNA-26a-5p. Chin Med J 2020;133:1211–1220. doi: 10.1097/CM9.0000000000000758